

Title:	Power Hardware-in-the-Loop Emulation of Permanent Magnet Synchronous Machines with Nonlinear Magnetics - Concept & Verification
Authors:	Alexander Schmitt, Jan Richter, Michael Braun, Martin Doppelbauer
Institute:	Karlsruhe Institute of Technology (KIT) Elektrotechnisches Institut (ETI)
Type:	Conference Proceedings
Published at:	Proceedings 2016 PCIM Europe, International Conference and Exhibition for Power Electronics, Intelligent Motion, Renewable Energy and Energy Management, Nuremberg, Germany, May 10-12, 2016 Publisher: VDE Verlag Year: 2016 ISBN: 978-3-8007-4186-1 Pages: 393-400

# Power Hardware-in-the-Loop Emulation of Permanent Magnet Synchronous Machines with Nonlinear Magnetics – Concept & Verification

Alexander Schmitt, Jan Richter, Michael Braun, Martin Doppelbauer  
 Institute of Electrical Engineering (ETI), Karlsruhe Institute of Technology (KIT)  
 Kaiserstraße 12, 76131 Karlsruhe, Germany, a.schmitt@kit.edu

## Abstract

This paper presents a power hardware-in-the-loop emulation test bench (PHIL), based on a modular multiphase multilevel converter (MMPMC), to mimic arbitrary permanent magnet synchronous machines with nonlinear magnetics as they are used in automotive applications. Measurements in stationary operation as well as high dynamic torque steps are conducted at a real automotive machine and precisely reproduced at the PHIL system to demonstrate the excellent performance of the PHIL test bench. Moreover, the superiority of a PHIL test bench over conventional motor test benches is proven by the unproblematic emulation of a blocking rotor or a cracking shaft.

## 1. Introduction

In modern automotive drive inverter development the importance of simulation increases rapidly. In early stage, various simulation tools are used to simulate and validate the accurate function of inverters. Afterwards, real-time hardware-in-the-loop test benches are used to test the developed software in conjunction with the signal processing unit of the power converter [1, 2, 3]. Finally, the converter has to be connected to a motor test bench to test and improve the performance, reliability or the manufacturing of the device. Unfortunately, there are several drawbacks inherent to conventional motor test benches. The inverter can only be tested when the motor is already available, which is usually not the case. Moreover, exchanging motors is extensive and several test benches are needed to cope with different power demands. Thus, the space required for test beds can be large and additional costs and maintenance efforts are caused. Furthermore, conventional motor test benches are limited in their fault emulation capability. Faults like a crack of the shaft, a blocking rotor or winding short circuits are very difficult to test. Therefore, it is desirable to connect the converter to a power hardware-in-the-loop (PHIL) emulation test bench (see Figure 1) to evaluate its proper function in all possible operating conditions. Such a device can mimic any machine using parameters that can be easily calculated by measurement or finite element analysis. Changing the motor type or data set can be executed by software within seconds.

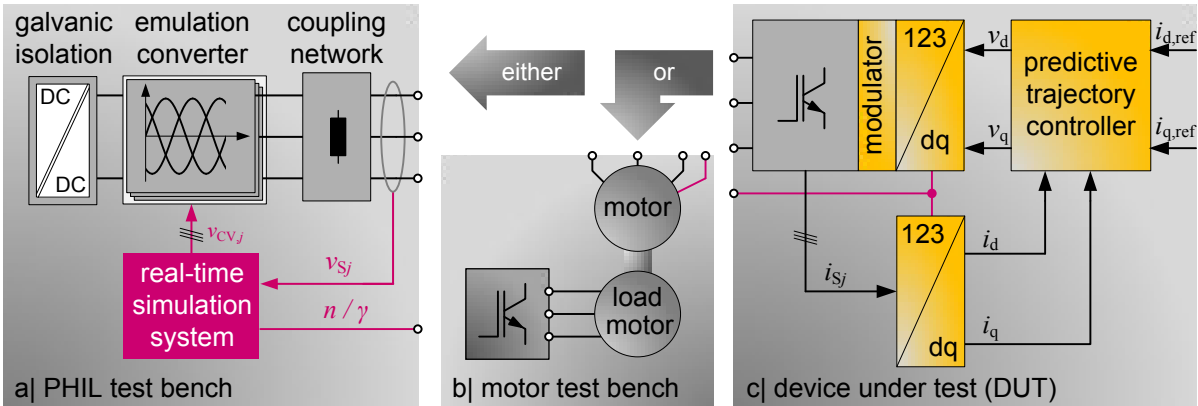


Figure 1: Either a motor test bench or a PHIL system can be used to test drive converters.

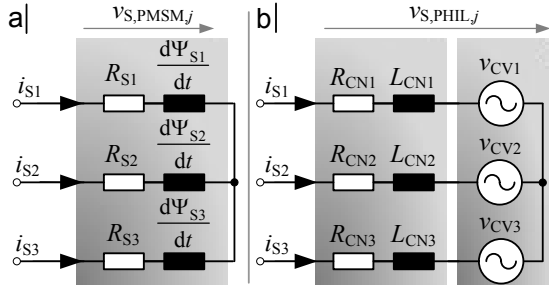


Figure 2: Equivalent circuit of a PMSM (a) and of the power hardware-in-the-Loop test bench (b).

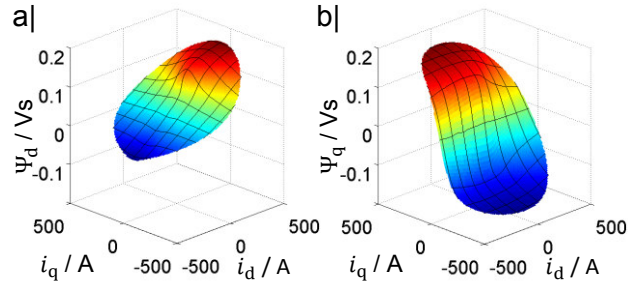


Figure 3: Flux linkage  $\Psi_d = f(i_d, i_q)$  (a) and flux linkage  $\Psi_q = f(i_d, i_q)$  (b) of the PMSM [5].

This paper presents a PHIL test bench and its application to permanent magnet synchronous machines with nonlinear magnetics for automotive applications. Because the PHIL test bench was already introduced in [4], this paper focuses on the verification and accuracy of the PHIL system. Indeed, for comprehension issues the theory of the underlying machine model [5] is briefly described in section 2. Subsequently, Section 3 summarizes the emulation concept and the used control scheme of the PHIL test bench [4]. Afterwards, the hardware setup for the verification is presented (Section 4) and the PHIL test bench is verified by means of stationary and dynamic measurements using a predictive trajectory dead-beat current controller (Section 5). Conclusions are stated in Section 6.

## 2. Theory

The proposed PHIL test bench consists of an emulation converter connected to the device under test (DUT) by means of an inductive coupling network (see Figure 1). The objective of a PHIL system is that the electrical behavior of the PHIL is identical to the real machine. Therefore, a machine model is required that describes the behavior of nonlinear permanent magnet synchronous machines considering the voltage drop at the coupling network. Figure 2 opposes the equivalent circuit of a PMSM and the equivalent circuit of the PHIL test bench. Nonlinear models of saturated, anisotropic permanent magnet synchronous machines are available and employed in this contribution [6]. The stator voltages  $v_{Sj}$ , with  $j \in \{1,2,3\}$  as phase numbers, can be calculated by employing Ohm's law, Faraday's law of induction and Kirchhoff's laws to the machine coils. This leads to:

$$v_{S,PMSM,j} = R_{Sj} \cdot i_{Sj} + \frac{d\Psi_{Sj}}{dt} \quad (1)$$

Since the characteristics of the PHIL test bench should be identical to the real PMSM, the phase voltages of the PHIL system must be identical to the phase voltages of the real machine [5]. This can be obtained by subtracting the voltage drop of the coupling network from the derivatives of the stator flux linkages and leads to:

$$v_{S,PMSM,j} = v_{S,PHIL,j} = R_{CNj} \cdot i_{Sj} + L_{CNj} \cdot \frac{di_{Sj}}{dt} + \underbrace{\left( \frac{d\Psi_{Sj}}{dt} - L_{CNj} \cdot \frac{di_{Sj}}{dt} - (R_{CNj} - R_{Sj}) \cdot i_{Sj} \right)}_{v_{CVj}} \quad (2)$$

Subsequent transformation to the rotor-fixed dq-reference frame yields:

$$v_d = R_{CN} \cdot i_d + L_{CN} \frac{di_d}{dt} - \omega \cdot L_{CN} \cdot i_q + \left( \frac{d\Psi_d}{dt} - \omega \Psi_q - L_{CN} \frac{di_d}{dt} + \omega \cdot L_{CN} \cdot i_q - (R_{CN} - R_S) \cdot i_d \right) \quad (3)$$

$$v_q = R_{CN} \cdot i_q + L_{CN} \frac{di_q}{dt} + \omega \cdot L_{CN} \cdot i_d + \left( \frac{d\Psi_q}{dt} + \omega \Psi_d - L_{CN} \frac{di_q}{dt} - \omega \cdot L_{CN} \cdot i_d - (R_{CN} - R_S) \cdot i_q \right) \quad (4)$$

There,  $R_S$  denotes the stator resistance,  $\omega$  the electric frequency,  $t$  the time and  $v_x$ ,  $i_x$  and  $\Psi_x$  the voltages, currents and flux linkages in the direct and quadrature axes ( $x \in \{d, q\}$ ). Furthermore,  $R_{CN}$  and  $L_{CN}$  are the resistance and the inductance of the coupling network. The required model parameters are the resistance  $R_S$  and the flux linkages  $\Psi_d$  and  $\Psi_q$  that depend nonlinearly on the currents  $i_d$  and  $i_q$  as defined by the function  $f$  and shown in Figure 3.

$$f: \mathbb{R}^2 \rightarrow \mathbb{R}^2, (i_d, i_q) \mapsto (\Psi_d, \Psi_q) \quad (5)$$

The model parameters can be obtained by finite-element method calculations [6] or by stationary measurements of the machine [7]. The machine model is used in a real-time simulator as illustrated in Figure 1 to calculate the counter voltages  $v_{CV,j}$  of the MMPMC so that the PHIL behaves exactly like the real motor [4]. Therefore the output voltages  $v_x$  of the DUT inverter are measured. Using (3) and (4), the derivatives of the machine currents can be calculated to:

$$\frac{di_d}{dt} = \frac{v_d - R_S i_d + \frac{L_{dq}}{L_{qq}}(-v_q + R_S i_q + \omega \Psi_d) + \omega \Psi_q}{L_{dd} - \frac{L_{dq} \cdot L_{qd}}{L_{qq}}} \quad (6)$$

$$\frac{di_q}{dt} = \frac{v_q - R_S i_q + \frac{L_{qd}}{L_{dd}}(-v_d + R_S i_d - \omega \Psi_q) - \omega \Psi_d}{L_{qq} - \frac{L_{dq} \cdot L_{qd}}{L_{dd}}} \quad (7)$$

Therein  $L_{xy}$  are differential inductances and thus partial derivatives of the flux linkage function in the direct and quadrature direction ( $x, y \in \{d, q\}$ ). The counter voltages of the MMPMC  $v_{CV,d}$  and  $v_{CV,q}$  can then be calculated by:

$$v_{CV,d} = \frac{di_d}{dt} (L_{dd} - L_{CN}) + \omega \cdot L_{CN} \cdot i_q + L_{dq} \cdot \frac{di_q}{dt} - \omega \Psi_q - (R_{CN} - R_S) \cdot i_d \quad (8)$$

$$v_{CV,q} = \frac{di_q}{dt} (L_{qq} - L_{CN}) - \omega \cdot L_{CN} \cdot i_d + L_{qd} \cdot \frac{di_d}{dt} + \omega \Psi_d - (R_{CN} - R_S) \cdot i_q \quad (9)$$

### 3. PHIL Concept

A precise emulation requires a complete identical behavior at the terminals of the PHIL test bench compared to the real machine. Therefore, the PHIL has to apply the counter voltage  $v_{CV,j}$  at the coupling network very precise and with a minimal dead-time to ensure the correct current slopes  $\frac{di_x}{dt}$  of arbitrary machines within the coupling inductance. For this reason, the basic challenge of PHIL emulation is the calculation and generation of the counter voltage. Modern FPGAs and A/D-converters allow the calculation of the machine model including the counter voltage with sample rates  $f_M$  of more than 1.5 MHz quasi continuous in real-time [5]. Indeed, the counter voltage generation is more challenging, especially for high power applications. The counter voltages are discontinuous functions since the current slopes  $\frac{di_x}{dt}$  depend on the clocked output voltages  $v_x$  and are different in active as well as freewheeling states of the DUT [4]. Moreover, the phase inductance of the coupling network  $L_{CN}$  can not correspond to the differential inductances  $L_{xy}$  of the machine (8), (9) due to iron saturation or the magnetic anisotropy of the rotor. For this reason, modelling of the current slopes requires a converter topology that allows a high dynamic and very precise generation of the counter voltages  $v_{CV,j}$ . The modular multiphase multilevel converter (MMPMC) [8] and the associated modulation scheme [9] offers such a dynamic and precise voltage generation and is used in this PHIL test bench. The schematic diagram of the entire PHIL test bench is shown in Figure 4. A MMPMC with  $n = 6$  branches per phase is used to generate a seven level output voltage waveform with a resulting PWM-frequency of  $f_{PWM} = 120$  kHz [9]. The MMPMC has

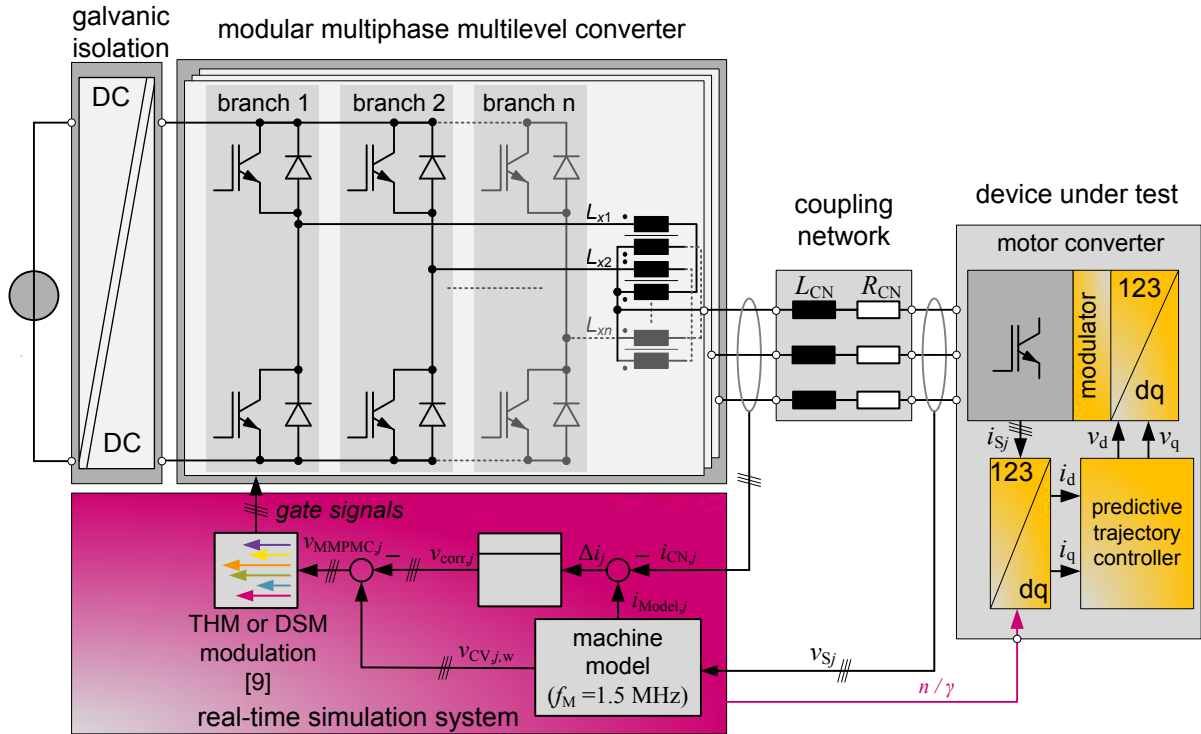


Figure 4: Detailed schematic diagram of the proposed PHIL test bench including the modular multiphase multilevel converter and the real-time simulation system as well as the coupling network and the device under test [4].

to be fed by a galvanic isolated DC-DC-converter because the real machine coils are also galvanically isolated. Furthermore, an external coupling network is necessary to connect the DUT inverter to the PHIL test bench since the MPPMC has the behavior of a voltage source. The real-time simulation system is based on an FPGA [5]. This FPGA contains the machine model, derived in Section 2, as well as the modulation of the MPPMC [9]. Since the counter voltage generation has unavoidable inaccuracies e.g. dead-times, forward voltages, zero current clamping etc. the real-time simulation system contains an additional P-controller. This P-controller is necessary to avoid a drift of the inner model currents  $i_{Model,j}$  and the real currents  $i_{CN,j}$ . A difference between the model and the real currents would affect the calculation of the counter voltages and the inner torque. Hence, it would distort the behavior of the PHIL test bench compared to the real machine [4]. Indeed, a simple P-controller is sufficient and does not affect the stability of the current controller of the DUT. In addition, the real-time simulation system is able to emulate an incremental encoder as well as a resolver. Identically to real machines, this sensor signal is the only connection between PHIL and DUT besides the three power terminals (Figure 4) [4].

#### 4. Experimental Setup

An interior permanent magnet synchronous machine for automotive traction applications of type *Brusa HSM1-6.1712-CO1* is used as a test motor (Figure 5 (b)). The machine has strongly nonlinear magnetics as can be seen in Figure 3, a maximum shaft power of 97 kW at a torque of 220 Nm and a rotor speed of  $4200 \text{ min}^{-1}$  (see. Table 1). Furthermore, Figure 5 (c) shows the DUT to control the test motor as well as the PHIL test bench. The motor converter is based on a *Semikron SkiiP (513GD122-3DUL)* six-pulse bridge and can be optionally connected to the motor (Figure 5 (b)) or the PHIL test bench (Figure 5 (a)). All measurements are carried out at a DC-link voltage of 300 V at the DUT and a DC-link voltage of 650 V at the MPPMC. Furthermore, a coupling inductance of  $L_{CN} = 1 \text{ mH}$  is used inside

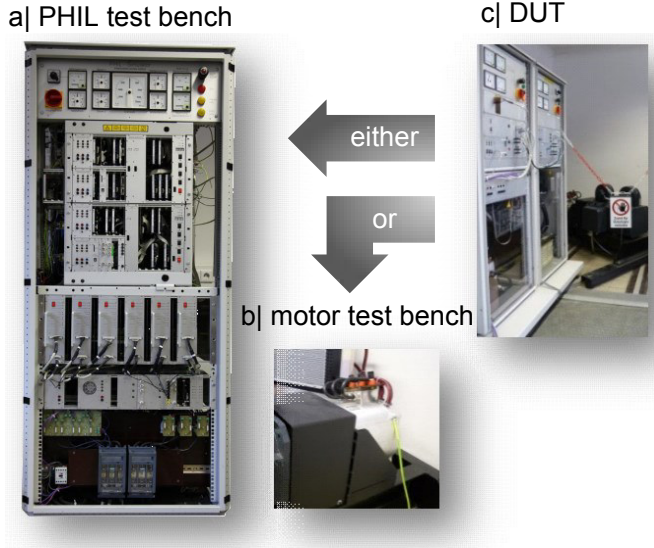


Table 1

Machine Parameters	
Parameter	Value
line voltage nom.	212 V
current nom. /max.	169 A / 300 A
shaft power nom. / max.	57 kW / 97 kW
number of pole pairs	3
torque nom. / max.	130 Nm / 220 Nm
speed nom. / max.	4200 min <sup>-1</sup> / 11000 min <sup>-1</sup>
$L_{dd}(0 \text{ A}, 0 \text{ A}) /$	410 $\mu\text{H}$ /
$L_{dd}(-200 \text{ A}, 200 \text{ A})$	204.5 $\mu\text{H}$
$L_{qq}(0 \text{ A}, 0 \text{ A}) /$	2.1 mH /
$L_{qq}(-200 \text{ A}, 200 \text{ A})$	163.6 $\mu\text{H}$

Figure 5: Test bench setup including the PHIL test bench (a), the real PMSM (b) and the DUT (c) [4].

the PHIL test bench. The test motor is set to a constant rotational speed of  $n = 1000 \text{ min}^{-1}$  by means of a speed controlled load motor which is connected to the PMSM. The rotational speed of the virtual machine was set to  $n = 1000 \text{ min}^{-1}$  by software. Furthermore, the current controller of the DUT is executed with a control and switching frequency of  $f_c = 8 \text{ kHz}$ . The real-time simulation system calculates the machine model with a sampling rate of  $f_M = 1.5 \text{ MHz}$  which is why the counter voltages are first averaged over one modulation period  $T_{\text{PWM}}$ . Afterwards, the threshold modulation [9] generates the counter voltage with a PWM frequency of  $f_{\text{PWM}} = 120 \text{ kHz}$ .

## 5. Results and Discussion

A predictive trajectory dead-beat controller as proposed in [7] is applied to control the motor converter. During the measurements, the integral component of the current controller was disabled. This ensures that dynamic as well as stationary variations between the PHIL test bench and the real motor are not compensated by the integral component. Thus, only the model accuracy of the PHIL test bench determines the accuracy of the current controller. Subsequently, the measurement results at the test motor and the PHIL test bench can be compared to precisely analyze the quality of the PHIL test bench.

### 5.1 Stationary Measurements

First, stationary measurements within the current plane were conducted at the PHIL test bench and at the test motor. Figure 6 shows the difference  $\varepsilon_x$  of the measured currents  $i_x$ .

$$\varepsilon_x = i_{x,\text{PHIL}} - i_{x,\text{PMSM}} \quad (10)$$

Note the current plane is currently limited to  $|i_x| < 200 \text{ A}$  due to the hardware limits of the PHIL test bench. The differences  $\varepsilon_q$  in the q-axis are illustrated in Figure 6 (a) and the differences in the d-axis  $\varepsilon_d$  are depicted in Figure 6 (b). The measured points are marked by dots in the diagram and the remaining points are interpolated on the basis of the measured values. The plots depict the excellent stationary performance of the PHIL test bench since the differences between the measured currents are  $\varepsilon_x < 2 \text{ A}$  in a wide operating range. Indeed, the difference between motor test bench and PHIL emulation system increases with increasing current caused by inaccuracies of the PHIL measurement and the counter voltage generation.

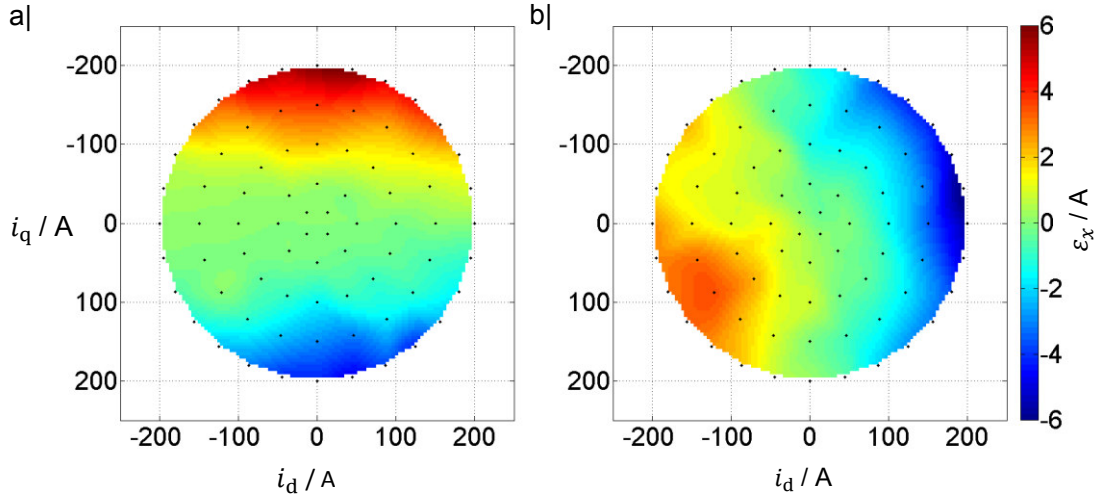


Figure 6: Difference between the q-currents (a) and the d-currents (b) at the PHIL test bench and the real motor during stationary operation.

## 5.2 Dynamic Measurements

The dynamic validation is conducted by a comparison of torque steps, shown in Figure 7. Thereby, a torque step from  $M_i = 0 \text{ Nm}$  to  $M_i = 100 \text{ Nm}$  is executed using three different control strategies at the DUT. The inductance of the d-axis is significant smaller than the inductance of the q-axis ( $L_{dq,0A} \approx 5 \cdot L_{dd,0A} \approx 2 \text{ mH}$ ) for this reason the d-axis offers significant higher current changes (see Table 1). This property can be used by high performance current controllers to optimize their strategies how a set value is reached. The left column of Figure 7 depicts the torque step for a direct current connection (DCC) of the set values (straight line), the middle column shows the short time to reference value strategy (STRV) which is the fastest way to reach the set value. Finally, the right column illustrates the fast torque response (FTR) trajectories. Therefore, the current jumps as fast as possible to the constant torque line to reach the requested torque and moves then along the constant torque line to the set value [7]. The torque steps are compared in the current plane (first row) as well as in their time response (second row). Finally the differences  $\varepsilon_x$  of the sampled values are calculated (third row). It can be seen that the PHIL precisely reproduces the dynamic q-current trend independent from the control strategy with variations of less than  $\varepsilon_{q,\max} < 10 \text{ A}$ . In the d-axis the currents are at the beginning also very similar but differ dependent on the control strategy in maximum between  $\varepsilon_{d,\max,\text{STRV}} \approx 10 \text{ A}$  and  $\varepsilon_{d,\max,\text{DCC}} \approx 25 \text{ A}$ . Indeed, these differences are not caused by modelling errors of the machine but by the limited output voltage of the PHIL test bench. A sufficient voltage reserve is essential since the machine inductance  $L_{dd}$  is significant smaller than the coupling inductance  $L_{CN}$ . Due to this, high counter voltages are necessary to generate the desired current slope  $\frac{di_d}{dt}$  within the coupling network (see eq. (8)). Otherwise, the dynamic of the current  $i_{d,\text{PHIL}}$  is limited in case that the output voltage is limited. For this reason, the possible machine inductance, the precision of the counter voltage generation and the DC-link voltage of the emulation converter have to be considered for the design of the coupling inductance. However, if the PHIL system operates within its maximum voltage, it emulates the machine nearly perfect.

## 5.3 Fault Emulation

Finally, the PHIL test bench is used to emulate fault conditions which cannot be tested at a real motor test bench. Figure 8 (a) depicts the emulation of a blocking rotor. Therefore, the rotational speed is abruptly set from  $n = 1000 \text{ min}^{-1}$  to  $n = 0 \text{ min}^{-1}$  at  $t = 0$ . The set value for the load torque is held constant at  $M_i = 75 \text{ Nm}$ . In contrast, Figure 8 (b) shows a step of

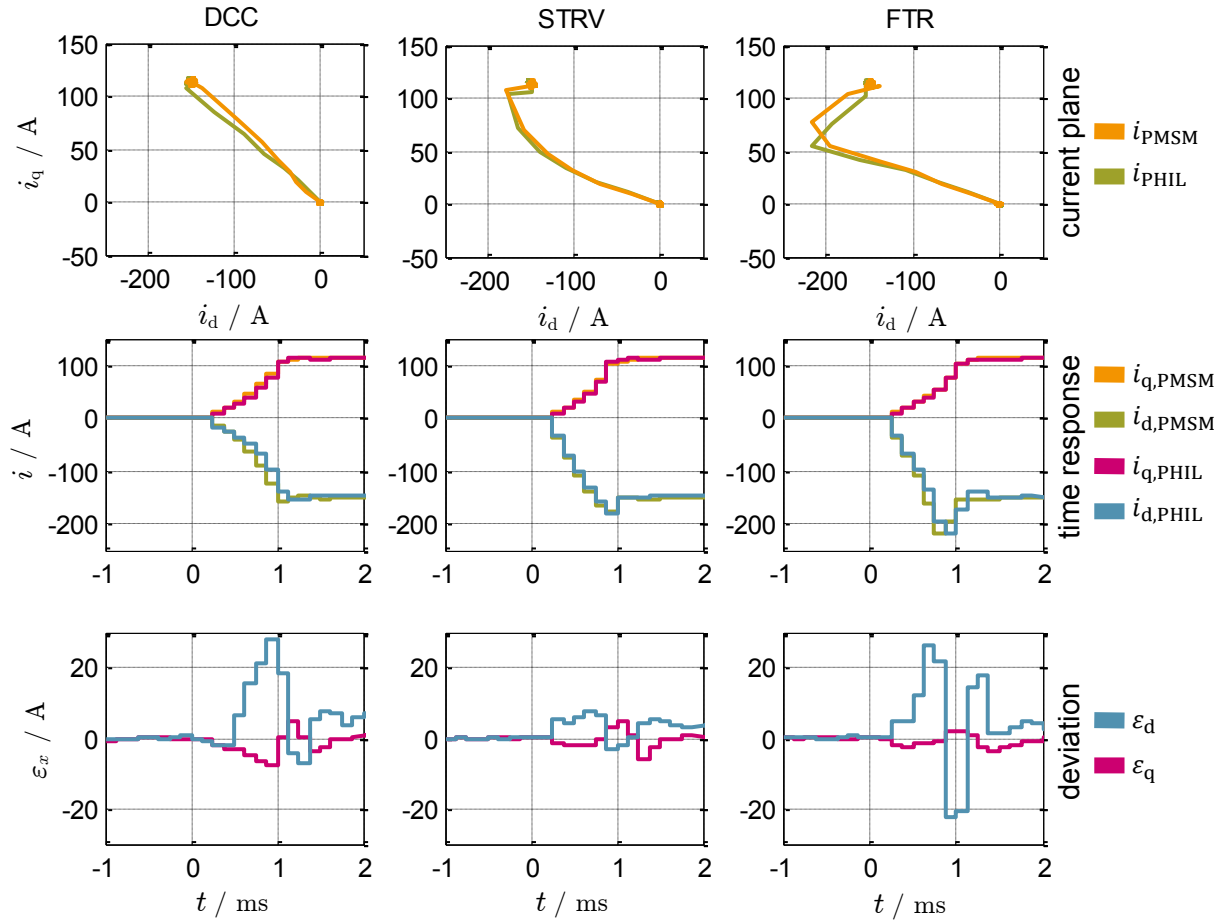


Figure 7: Torque step from  $M_i = 0 \text{ Nm}$  to  $M_i = 100 \text{ Nm}$  for three different control strategies: Direct Current Connection DCC (left column), Short Time to Reference Values STRV (middle column) and Fast Torque Response FTR (right column) [7].

the rotational speed from  $n = 1000 \text{ min}^{-1}$  to  $n = 2000 \text{ min}^{-1}$  at  $t = 0$  whereas the load torque is  $M_i = 25 \text{ Nm}$ . Such a step can occur when the inertia torque suddenly decreases e.g. due to a cracking shaft. However, a blocking rotor or a change of the inertia torque cannot be tested with conventional motor test benches. Indeed, since the validity of the PHIL test bench is already proven, the PHIL test bench allows reliable tests of the DUT in operating points that are not possible on conventional motor test benches. This underlines the superiority of a PHIL test bench over conventional motor test benches in automotive drive development processes.

## 6. Conclusion

This paper has presented a power hardware-in-the-loop emulation test bench (PHIL), based on a modular multiphase multilevel converter (MMPMC), to mimic arbitrary permanent magnet synchronous machines with nonlinear magnetics. The underlying machine model as well as the PHIL concept using a seven level modular multiphase multilevel converter is introduced and verified. Therefore, the PHIL test bench is parametrized for an automotive PMSM and controlled by a DUT using a predictive trajectory dead-beat current controller. Measurements in stationary operation as well as high dynamic torque steps are conducted at a real automotive motor and precisely reproduced at the PHIL system and demonstrate the excellent performance of the PHIL test bench. Furthermore, the superiority of a PHIL test



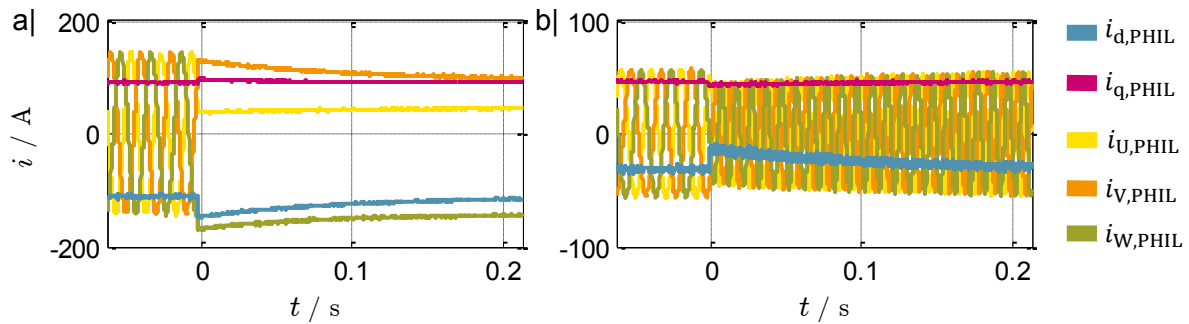


Figure 8: Emulation of a rotational speed step from 1000  $\text{min}^{-1}$  to 0  $\text{min}^{-1}$  (a) and from 1000  $\text{min}^{-1}$  to 2000  $\text{min}^{-1}$  (b)

bench over conventional motor test benches in automotive drive development processes is proven by the unproblematic emulation of a blocking rotor or a cracking shaft.

## References

- [1] C. Dufour, S. Cense, T. Yamada, R. Imamura, and J. Belanger, "Fpga permanent magnet synchronous motor floating-point models with variable-dq and spatial harmonic finite-element analysis solvers," in *15th International Power Electronics and Motion Control Conference (EPE/PEMC)*, 2012, pp. LS6b.2–1–LS6b.2–10.
- [2] M. Matar and R. Iravani, "Massively parallel implementation of ac machine models for fpga-based real-time simulation of electromagnetic transients," *IEEE Transactions on Power Delivery*, vol. 26, no. 2, pp. 830–840, Apr. 2011.
- [3] L. Herrera and J. Wang, "Fpga based detailed real-time simulation of power converters and electric machines for ev hil applications," in *IEEE Energy Conversion Congress and Exposition (ECCE)*, Sept. 2013, pp. 1759–1764.
- [4] A. Schmitt, J. Richter, M. Gommeringer, T. Wersal, and M. Braun, "A novel 100 kw power hardware-in-the-loop emulation test bench for permanent magnet synchronous machines with nonlinear magnetics," in *8th IET International Conference on Power Electronics, Machines and Drives (PEMD 2016)*, Glasgow, Apr. 2016, pp. 1–6.
- [5] A. Schmitt, J. Richter, U. Jurkewitz, and M. Braun, "FPGA-based real-time simulation of nonlinear permanent magnet synchronous machines for power hardware-in-the-loop emulation systems," in *IECON 2014 - 40th Annual Conference of the IEEE Industrial Electronics Society*, Oct. 2014, pp. 3763–3769.
- [6] X. Chen, J. Wang, B. Sen, P. Lazari, and T. Sun, "A high-fidelity and computationally efficient model for interior permanent-magnet machines considering the magnetic saturation, spatial harmonics, and iron loss effect," *IEEE Transactions on Industrial Electronics*, vol. 62, no. 7, pp. 4044–4055, Jul. 2015.
- [7] J. Richter, P. Bauerle, T. Gemassmer, and M. Doppelbauer, "Transient trajectory control of permanent magnet synchronous machines with nonlinear magnetics," in *IEEE International Conference on Industrial Technology (ICIT)*, Mar. 2015, pp. 2345–2351.
- [8] A. Schmitt, M. Gommeringer, J. Kolb, and M. Braun, "A high current, high frequency modular multiphase multilevel converter for power hardware-in-the-loop emulation," in *International Exhibition and Conference for Power Electronics, Intelligent Motion, Renewable Energy and Energy Management; Proceedings of PCIM Europe*, May 2014, pp. 1537–1544.
- [9] A. Schmitt, M. Gommeringer, C. Rollbühler, P. Pomnitz, and M. Braun, "A novel modulation scheme for a modular multiphase multilevel converter in a power hardware-in-the-loop emulation system," in *IECON 2015 - 41st Annual Conference of the IEEE Industrial Electronics Society*, Nov. 2015, pp. 1276–1281.